

Real-time shot-noise-limited differential photodetection for atomic quantum control

F. Martin Ciurana,¹ G. Colangelo,¹ Robert J. Sewell,¹ and M.W. Mitchell^{1,2}

¹ICFO – Institut de Ciències Fotoniques, Av. Carl Friedrich Gauss, 3, 08860 Castelldefels, Barcelona, Spain

²ICREA – Institució Catalana de Recerca i Estudis Avançats, 08015 Barcelona, Spain

(Dated: May 12, 2016)

We demonstrate high-efficiency, shot-noise-limited differential photodetection with real-time signal conditioning, suitable for feedback-based quantum control of atomic systems. The detector system has quantum efficiency of 0.92, is shot-noise limited from 7.4×10^5 to 3.7×10^8 photons per pulse, and provides real-time voltage-encoded output at up to 2.3 Mpulses per second.

Feedback control of atomic quantum systems [1] enables quantum information protocols including deterministic teleportation [2], stabilization of non-classical states [3], entanglement generation [4, 5] and quantum-enhanced sensing [6, 7]. Efficient closed-loop control has been achieved by combining optical quantum non-demolition (QND) measurement [8, 9] with electromagnetic [10] or optical [11] feedback. Fidelity of these protocols requires speed, sensitivity and low disturbance in the QND measurement [12]. Because advanced QND techniques such as two-color probing [13] and two-polarization probing [14] address specific hyperfine transitions, this also requires small (\sim GHz) detunings, and thus low photon numbers to achieve low disturbance. This combination of requirements in the measurement places multiple demands on the detectors used in the QND measurement.

Here we present a balanced differential photodetector (DPD) suitable for $\sim \mu$ s pulsed Faraday rotation [15] and two-color [13] dispersive probing of atomic ensembles with sensitivity and dynamic range comparable to the best published differential detectors [16, 17]. The DPD employs $> 90\%$ quantum efficiency photodiodes and charged-particle-detection amplifiers. Real time output is achieved with low-noise sample and hold amplifiers (SHAs) and a differential amplifier (DA). The system enables atomic quantum control in which feedback to an atomic system must be accomplished with a sub- μ s loop time [11, 18].

The electronics for the DPD and DA together with the test setup are shown schematically in Fig. 1. The detector consists of two PIN photo-diodes (PDs) (Hamamatsu S3883) connected in series and reverse biased by 5 V to improve their response time. The differential output current is DC coupled to the integrator, a very low noise charge-sensitive pre-amplifier (Cremat CR-110) with a capacitor C_i and a discharge resistor R_i in the feedback branch. Together these determine the relaxation time constant $\tau = R_i C_i = 290 \mu$ s of the integrator. The 50 ns rise-time of the circuit is limited by the capacitance of the photodiodes while the CR-100 itself has a nominal rise time of 7 ns. Pulses longer than the rise time but shorter than the relaxation time produce a step in the output voltage proportional to N_{diff} , the difference of photon numbers

on the two photodiodes. The output from the DPD is captured by a pair of sample and hold amplifiers (SHAs) (Analog Devices AD783), gated with TTL signals. The SHA1 captures the voltage of the DPD before the optical pulse arrives, and SHA2 captures it after the end of the pulse. A differential amplifier (DA) (Analog Devices AD8274) amplifies the difference of the two voltages held on the SHAs.

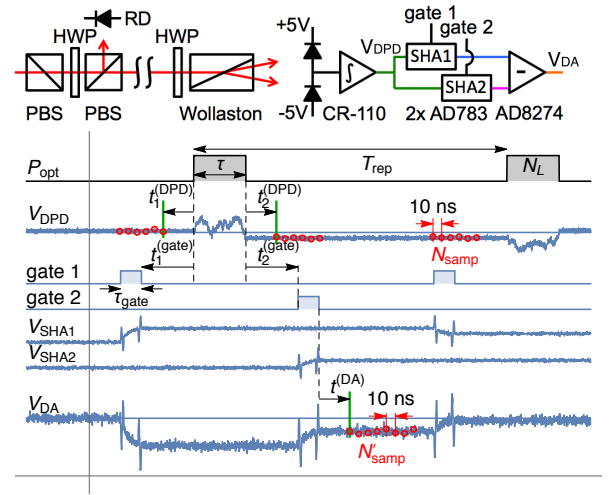


FIG. 1. Top: Schematic of the optics and detector electronics. A laser and acousto-optic modulator (not shown) are used to produce pulses of desired duration and energy. A first polarizing beam splitter (PBS) is used to generate a well defined linear polarization, a half-wave plate (HWP) and second PBS are used to split a constant fraction of the pulse to a reference detector (RD). A HWP together with a Wollaston prism are used to balance the energies reaching the photodiodes, wired in series for direct current subtraction. A charge-sensitive pre-amplifier (Cremat CR-110) amplifies the difference current, and a pair of SHAs (Analog Devices AD783) sample the pre-amplifier output shortly before and shortly after the pulse. A differential amplifier (DA) (Analog Devices AD8274) outputs the difference of the two SHA signals. Bottom: Timing diagram of optical input, SHA gate voltages and DPD and DA signals, illustrating a possible response to two pulses of a pulse train. P_{opt} : optical power, V_{DPD} : Balanced detector output, gate 1, gate 2: gate voltages causing the respective SHAs to sample (high) and to hold (low), V_{DA} : differential amplifier output. Red circles show oscilloscope voltage samples use to characterize the DPD and DA noise characteristics.

To characterize the noise performance of the DPD we send trains of pulses with a desired photon number N , pulse duration τ , and pulse repetition period T_{rep} . We use a continuous-wave diode laser at 780 nm, chopped by an acousto-optic modulator and balanced by means of a half waveplate and Wollaston prism, as shown in Fig. 1. We record the reference detector (RD) and DPD output voltages on an 8-bit digital storage oscilloscope (LeCroy Waverunner 64Xi) at a sampling rate of 100 Msps which acquires samples continuously and asynchronously to the pulse generation. We define a single measurement for the DPD as $N_{\text{diff}} = C(\bar{V}_1 - \bar{V}_2)$, where $\bar{V}_1(\bar{V}_2)$ is the mean of N_{samp} voltage samples before (after) the optical pulse and C is a calibration factor. The number of photons N_{phot} in a pulse is estimated as $N_{\text{phot}} = C_{\text{RD}} \sum_i V_{\text{RD}}(t_i)$ where V_{RD} is the voltage output of RD. The sum is taken over the duration of the pulse and C_{RD} is a calibration factor obtained by comparison against a power meter. For a given set of conditions, we adjust the waveplate to give a balanced signal $N_{\text{diff}} \approx 0$ and record M pulses in a single pulse train, from which we extract M values for N_{diff} and N_{phot} and compute statistics.

When source and detector fluctuations are taken into consideration, a linear detector will have an output signal variance given by a second-order polynomial in the average optical input energy [19],

$$\text{var}N_{\text{diff}} = a_0 N_{\text{phot}}^0 + \eta N_{\text{phot}} + a_2 N_{\text{phot}}^2. \quad (1)$$

Here a_0 is the “electronic noise” (EN) contribution, $a_2 N_{\text{phot}}^2$ is the “technical noise” (TN) and the second term is the shot noise (SN) contribution with η the quantum efficiency of the detector. The different scalings with N_{phot} allow an unambiguous identification of the different noise contributions.

To estimate the coefficients of Eq.1 we collect data at a variety of N_{phot} in each case recording a train of 2500 pulses with repetition period $T_{\text{rep}} = 0.8 \mu\text{s}$ and pulse duration $\tau = 200 \text{ ns}$. Our light source is not powerful enough to measure the turning point from SN-limited to TN-limited. In order to estimate when the TN becomes the dominant source of noise we construct “composite pulses” containing a larger total number of photons by summing the signals from multiple pulses [20]. The measured variances are fitted with Eq. (1) to obtain a_0 , η and a_2 . We set $t_1^{(\text{DPD})} = 10 \text{ ns}$ to ensure that \bar{V}_1 is measuring the voltage before the detection of the optical pulse and $t_2^{(\text{DPD})} = 90 \text{ ns}$ which is the minimum time to sample $> 99\%$ of the DPD signal, with $N_{\text{samp}} = 10$ points. Typical results are shown in Fig. 2 (a). The detector is shot-noise limited when $a_0/\eta < N_{\text{phot}} < \eta/a_2$. From the fit outputs, see Fig. 2 for details, we determine that the DPD is SN-limited from $(4.06 \pm 0.07) \times 10^5 < N_{\text{phot}} < (3.97 \pm 2.18) \times 10^9$ photons, i.e., its SN limited behavior extends over 4 orders of magnitude.

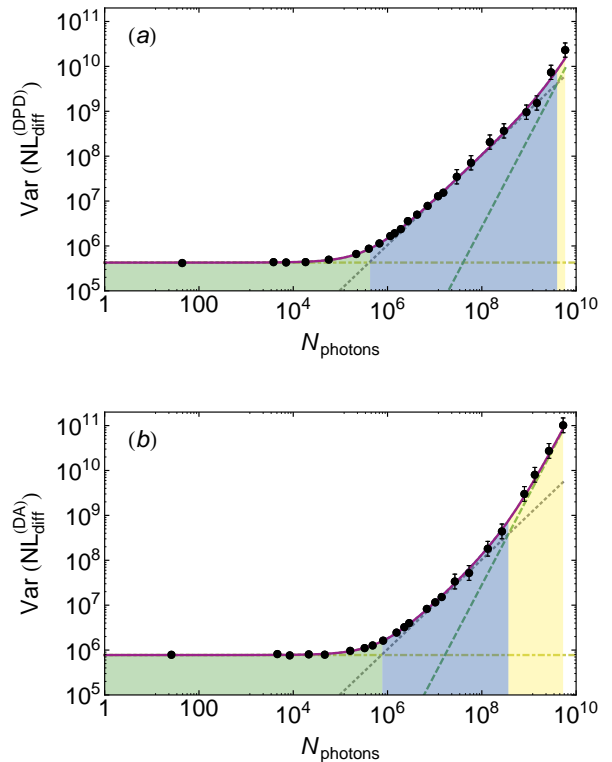


FIG. 2. Variance of the output signal of the DPD (a) and DA (b) as function of the input photon-number in log-log scale. Solid red line fit to $\text{Var}(NL_{\text{diff}})$ using expression Eq.1. Shaded areas depicts the different detection responses: green EN-limited, blue SN-limited and yellow TN-limited. Error bars represent $\pm 1\sigma$ standard error. For both devices $T_{\text{rep}} = 0.8 \mu\text{s}$ and $\tau = 200 \text{ ns}$. (a): $\text{var}N_{\text{diff}}^{\text{DPD}}$ as function of the N_{phot} . Analysis done with $t_1^{(\text{DPD})} = 10 \text{ ns}$, $t_2^{(\text{DPD})} = 90 \text{ ns}$ and $N_{\text{samp}} = 10$ points. The yellow line dot-dashed is the electronic noise level, $a_0 = (4.26 \pm 0.05) \times 10^5$, the dotted gray line is the shot-noise term, $\eta = 1.05 \pm 0.01$, and the dashed green line is the technical noise contribution, $a_2 = (2.64 \pm 1.45) \times 10^{-10}$. (b): $\text{var}N_{\text{diff}}^{\text{DA}}$ as function of the N_{phot} . The timings for the gates of the SHAs are $t_1^{(\text{gate})} = 10 \text{ ns}$, $t_2^{(\text{gate})} = 20 \text{ ns}$ with analysis parameters $t^{(\text{DA})} = 170 \text{ ns}$ and $N'_{\text{samp}} = 10$ points. The yellow line dot-dashed is the EN level, $a_0 = (7.75 \pm 0.09) \times 10^5$, the dotted gray line is the SN term, $\eta = 1.04 \pm 0.01$, and the dashed green line is the TN contribution, $a_2 = (2.84 \pm 0.70) \times 10^{-9}$.

To characterize the noise properties of the DA we repeat the same procedure as for the DPD: we record on the oscilloscope the RD and DA output voltages. The SHA1 captures $V_{\text{DPD}}(t_1^{(\text{gate})})$ before the optical pulse arrives, and the SHA2 captures $V_{\text{DPD}}(t_2^{(\text{gate})})$ after the end of the pulse, analogous to \bar{V}_1 and \bar{V}_2 , respectively. We define a single measurement as $N_{\text{diff}} = C'\bar{V}_{\text{DA}}$, where \bar{V}_{DA} is the mean of N'_{samp} voltage samples a time $t^{(\text{DA})}$ after the end of the SHA2 and C' is a calibration factor obtained by comparison against a power meter. Under the same experimental conditions, $T_{\text{rep}} = 0.8 \mu\text{s}$ and $\tau = 200 \text{ ns}$, we record a train of 2500 pulses for each value

of N_{phot} and fit $\text{var}N_{\text{diff}}^{(\text{DA})}$ with Eq. (1) we obtain a_0 , η and a_2 . As before, we construct “composite pulses” to determine a_2 . The SHAs are gated for $\tau_{\text{gate}} = 100$ ns at times $t_1^{(\text{gate})} = 10$ ns and $t_2^{(\text{gate})} = 20$ ns. The analysis parameters are $t^{(\text{DA})} = 170$ ns and $N'_{\text{samp}} = 10$ points. Typical results are shown in Fig. 2 (b). From the fit outputs we determine that the DA is shot-noise limited from $(7.43 \pm 0.14) \times 10^5 < N_{\text{phot}} < (3.67 \pm 0.91) \times 10^8$ photons, i.e., over almost 3 orders of magnitude.

From the coefficients a_0 we can deduce the noise-equivalent charge (NEC), the number of photo-electrons necessary to create a signal equivalent to the electronic noise $q_{\text{SN}} = \eta_Q \sqrt{N_{\text{phot, SN}}}$ for the DPD and for the DA. The quantum efficiency of the photo-diodes in the detector at 780nm is $\eta_Q = 0.92$, resulting in $\text{NEC}^{\text{DPD}} = 600$ electrons and $\text{NEC}^{\text{DA}} = 808$ electrons. Since the two calibration experiments were taken under the same experimental conditions, i.e., $T_{\text{rep}} = 0.8 \mu\text{s}$ and $\tau = 200$ ns, and comparable analysis conditions $\tau_{\text{gate}} = 100$ ns and $N_{\text{samp}} = N'_{\text{samp}} = 10$ points, we see that the capability of having the signal available in real time has the cost of increasing the electronic noise level by 1.3dB.

The electronic noise of DPD contains high-bandwidth noise, e.g. Johnson noise, that can be reduced by averaging the in-principle constant output over a time window, which could be longer than the pulse itself. On the other hand, longer windows will be more sensitive to drifts and “ $1/f$ ” noise. We investigate this trade-off by changing N_{samp} used to obtain \bar{V}_1 and \bar{V}_2 and then fit $\text{var}N_{\text{diff}}^{(\text{DPD})}$ with Eq.1 to get a_0 , η and a_2 . The experiment is done at $T_{\text{rep}} = 30 \mu\text{s}$ and $\tau = 200$ ns, and the analysis with $t_1^{(\text{DPD})} = 10$ ns and $t_2^{(\text{DPD})} = 90$ ns. For each N_{phot} we record more than 300 pulses in a single pulse train. From these parameters we evaluate the SN limited region of the DPD as a function of the measurement bandwidth. We fit the EN (TN) limited region $a_0/\eta < N_{\text{phot}}$ ($N_{\text{phot}} > \eta/a_2$) with the polynomial $\alpha_1 N_{\text{samp}}^{\beta_1} + \alpha_2 N_{\text{samp}}^{\beta_2}$ (Eq.2), where the two terms are for the two noise time-scales.

In Fig. 3 we observe a transition from $\text{EN} \propto N_{\text{samp}}^{\beta_1}$, where $\beta_1 < 0$ for $N_{\text{samp}} \lesssim 100$ points, describing the effects of averaging, to a $1/f$ regime for $N_{\text{samp}} \gtrsim 600$ points, with $\text{EN} \propto N_{\text{samp}}^{\beta_2}$ where $\beta_2 > 0$. The fit results are $\beta_1^{\text{EN DPD}} = -0.60 \pm 0.02$ and $\beta_2^{\text{EN DPD}} = 0.99 \pm 0.13$. We also notice that Fig. 3 shows that increasing N_{samp} from 1 point to 400 we can reduce the electronic noise of the DPD by 10.2dB, and that at 400 samples the DPD electronic noise is minimal with a NEC of 242 electrons corresponding to a measurement bandwidth of 125 kHz.

We repeat the measurement under the same scope settings to determine the electronic noise contribution of the scope itself terminating it with a 50Ω terminator. Analogously, we vary N_{samp} to obtain \bar{V}_1 and \bar{V}_2 and observe that the a_0^{scope} is negligible relative to a_0^{DPD} . The fact that $\beta_1^{\text{EN DPD}} = -0.60$ and not -1 (as in the case of

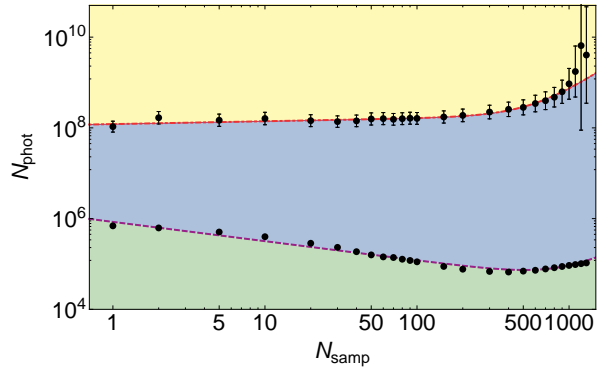


FIG. 3. DPD SN-limited region (blue area) as function of measurement bandwidth (N_{samp}) in log-log plot. EN-limited region (green) and TN-limited (yellow), see text for details. Experimental parameters $T_{\text{rep}} = 30 \mu\text{s}$ and $\tau = 200$ ns. Red dot-dashed curve is a fit of TN with Eq. 2 with results $\alpha_1^{\text{TN}} = (1.36 \pm 0.56) \times 10^8$, $\alpha_2^{\text{TN}} = (0.53 \pm 4.65) \times 10^3$, $\beta_1^{\text{TN}} = 0.03 \pm 0.11$ and $\beta_2^{\text{TN}} = 1.99 \pm 1.31$. Purple dashed curve is a fit of EN with Eq.2 with output values $\alpha_1^{\text{EN}} = (1.68 \pm 0.11) \times 10^6$, $\alpha_2^{\text{EN}} = 40 \pm 25$, $\beta_1^{\text{EN}} = -0.60 \pm 0.02$ and $\beta_2^{\text{EN}} = 1.08 \pm 0.09$. The scope “electronic noise” a_0 fit (not shown) has values $\alpha_1^{\text{scope}} = (3.79 \pm 0.47) \times 10^4$, $\alpha_2^{\text{scope}} = 0.17 \pm 0.16$, $\beta_1^{\text{scope}} = -0.96 \pm 0.03$ and $\beta_2^{\text{scope}} = 0.99 \pm 0.13$ and conclude that the scope noise contribution is negligible. Sample rate is 100 Msps or 10 ns/sample. Error bars represent $\pm 1\sigma$ standard error.

β_1^{scope}) means that there is some correlated noise in the DPD output signal. This is expected as the 100 MHz sampling frequency exceeds the oscilloscope input bandwidth at this setting. The measured -3 dB oscilloscope bandwidth is 30 MHz.

Even though the EN increases for $N_{\text{samp}} > 400$, the SN limited region i.e., the area between the EN and the TN curves, still increases with N_{samp} as the reduction of the TN-limited region compensates the increase of the EN. We can observe that the TN is almost flat for $N_{\text{samp}} \lesssim 300$ but rapidly decreases for $N_{\text{samp}} > 500$. The DPD is SN-limited over measurements bandwidth running from 3 MHz to 35 kHz.

The DPD presented here offers a significant improvement in speed compared to other state-of-the-art detectors, while also having somewhat lower noise [16, 17, 21]. In [17] two detectors based on two different charge-sensitive pre-amplifier are described with minimal $\text{ENC}=280$ (Amptek-based detector) and $\text{ENC}=340$ (Cremat-based detector) operated at speeds $\lesssim 200$ kHz (exact value not reported). Our DPD shows a minimal $\text{ENC}=242$ at 125 kHz, representing a noise improvement of 0.63dB (Amptek-based detector) and 1.84dB (Cremat-based detector) while operating at similar measurement bandwidth. Similarly, in [21] the maximum measurement speed is 200 kHz and SN limited starting from 10^6 photons/pulse (our DPD is SN limited from 7×10^4). Ref [16], working at a repetition rate of 1 MHz reports a NEC

of 730 electrons, whereas our DPD has a NEC of 600 electrons at 1 MHz, a reduction of 0.87 dB. Furthermore, our DPD has a minimum repetition period of $T_{\text{rep}}^{(\text{DPD})} = \text{DPD rise time (50 ns)} + t_1^{(\text{DPD})} (10 \text{ ns}) + t_2^{(\text{DPD})} (10 \text{ ns}) + 2 N_{\text{samp}} (2 \times 10 \text{ ns}) = 90 \text{ ns}$, or equivalently, a maximum detection bandwidth of 11 MHz, which to our knowledge makes it the fastest quantum-noise limited differential photodetector for this energy regime, i.e., for pulses with as few as 6.8×10^5 photons. Along with the speed, our DPD is SN limited over measurements bandwidth running from $\sim 10 \text{ MHz}$ to kHz.

Atomic experiments have coherence times running from μs to seconds requiring a real time detector with low latency and large bandwidth to perform many manipulations of the atomic state before decoherence occur. The maximum measurement speed of our DA is determined by τ_{gate} , the sampling time of the SHAs to faithfully capture V_{DPD} , and $t^{(\text{DA})}$, the settling time of the SHA once the sampling has been done.

We investigate the effect of τ_{gate} by measuring $\text{var} N_{\text{diff}}^{\text{DA}}$ vs N_{phot} for different values of τ_{gate} and compare the fit outputs. We obtain the same results for $\tau_{\text{gate}} = 250 \text{ ns}$, the manufacturer recommended value, as for $\tau_{\text{gate}} = 100 \text{ ns}$, with fit parameters comparable within the standard error, but not for 50 ns where the DA-output is independent of N_{phot} , i.e., dominated by EN.

We study the effect of the settling time of the SHA2 by varying the samples used for \bar{V}_{DA} with $t^{(\text{DA})}$ and fit $\text{var} N_{\text{diff}}^{(\text{DA})}$ to obtain the parameters a_0 , η and a_2 . From the fit outputs we determine the EN-limited and TN-limited regions. In Fig. 4 we see that for values of $t^{(\text{DA})}$ where the noise of the SHA has not had time to settle the EN and the TN contributions are large, dominant over SN. We also observe that once $t^{(\text{DA})}$ is sufficient, the EN region is flat as expected from the output of a the DA. From the fit outputs η we determine that the minimum value to have $> 99\%$ of the signal corresponds to $t^{(\text{DA})} = 170 \text{ ns}$.

The minimum time at which we can measure two consecutive pulses is given by $T_{\text{rep}}^{(\text{DA})} = \text{DPD rise time (50 ns)} + 2\tau_{\text{gate}} (2 \times 100 \text{ ns}) + t^{(\text{DA})} (170 \text{ ns}) + N'_{\text{samp}} (10 \text{ ns}) = 430 \text{ ns}$, or equivalently, the maximum detection bandwidth in real time is 2.3 Mpulses/s.

Comparing Fig. 2 and Fig. 4 we see that the SN-limited region is a bit narrower in Fig. 4, due to the different N'_{samp} used in the analysis. This suggests that the output of the DA has fast frequency noise components that could be filtered to obtain the same noise performance as in Fig. 2.

In conclusion, we have demonstrated a pulsed differential photodetector (DPD) and a detection system to make the signal available in real time. The DPD has bandwidth up to $\sim 11 \text{ MHz}$ which to our knowledge makes it the fastest quantum-noise limited differential photodetector for pulses with as few as 6.8×10^5 photons per pulse.

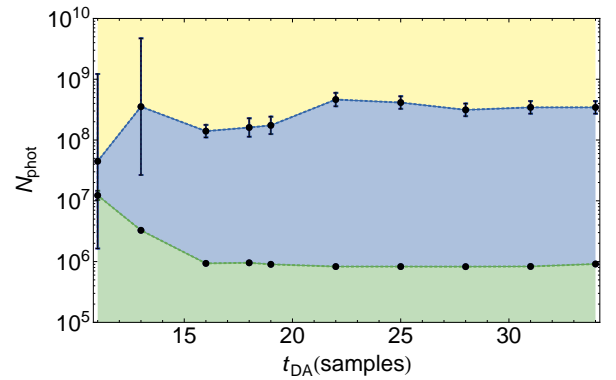


FIG. 4. DA SN-limited region (blue area) as function of the SHA2 settling time ($t^{(\text{DA})}$). Green shaded area is EN-limited region and TN-limited region in yellow, see text for details. Experimental parameters $T_{\text{rep}} = 0.8 \mu\text{s}$, $\tau = 200 \text{ ns}$, $t_1^{(\text{gate})} = 10 \text{ ns}$ and $t_2^{(\text{gate})} = 20 \text{ ns}$. Analysis done with $N'_{\text{samp}} = 1$ point at a sample rate of 100 Msp/s or 10 ns/sample. Error bars represent $\pm 1\sigma$ standard error.

We make the signal available in real time by using a pair of sample and hold amplifiers (SHA) and a differential amplifier (DA). The DA is shot noise limited per input pulses varying from 7.4×10^5 to 3.7×10^8 photons per pulse and shows low latency, 170 ns. The DPD together with the DA and can directly be employed in real time quantum control experiments with flexible measurement bandwidth varying from kHz up to 2.3 MHz.

We thank Patrick Windpassinger for help and insights in the detector design, and José Carlos Cifuentes for help with the electronics design and construction.

Work supported by the Spanish MINECO projects MAQRO (Ref. FIS2015-68039-P), EPEC (FIS2014-62181-EXP) and Severo Ochoa grant SEV-2015-0522, Catalan 2014-SGR-1295, by the European Research Council project AQUMET, Horizon 2020 FET Proactive project QUIC and by Fundació Privada CELLEX.

-
- [1] A. Serafini, ISRN Optics **2012**, 15 (2012), URL <http://dx.doi.org/10.5402/2012/275016>]
 - [2] J. F. Sherson, H. Krauter, R. K. Olsson, B. Julsgaard, K. Hammerer, I. Cirac, and E. S. Polzik, Nature **443**, 557 (2006), URL <http://dx.doi.org/10.1038/nature05136>.
 - [3] C. Sayrin, I. Dotsenko, X. Zhou, B. Peaudecerf, T. Rybarczyk, S. Gleyzes, P. Rouchon, M. Mirrahimi, H. Amini, M. Brune, et al., Nature **477**, 73 (2011), URL <http://dx.doi.org/10.1038/nature10376>.
 - [4] G. Toth and M. W. Mitchell, New J. Phys. **12** (2010), ISSN 1367-2630.
 - [5] N. Behbood, F. Martin Ciurana, G. Colangelo, M. Napolitano, G. Tóth, R. J. Sewell, and M. W. Mitchell, Phys. Rev. Lett. **113**, 093601 (2014), URL <http://link.aps.org/doi/10.1103/PhysRevLett.113>.

- 093601.
- [6] H. Yonezawa, D. Nakane, T. A. Wheatley, K. Iwasawa, S. Takeda, H. Arao, K. Ohki, K. Tsumura, D. W. Berry, T. C. Ralph, et al., *Science* **337**, 1514 (2012), ISSN 0036-8075, <http://science.sciencemag.org/content/337/6101/1514.full.pdf> URL <http://science.sciencemag.org/content/337/6101/1514>.
- [7] R. Inoue, S.-I.-R. Tanaka, R. Namiki, T. Sagawa, and Y. Takahashi, *Phys. Rev. Lett.* **110**, 163602 (2013), URL <http://link.aps.org/doi/10.1103/PhysRevLett.110.163602>.
- [8] R. J. Sewell, M. Napolitano, N. Behbood, G. Colangelo, and M. W. Mitchell, *Nat Photon* **7**, 517 (2013), URL <http://dx.doi.org/10.1038/nphoton.2013.100>.
- [9] O. Hosten, N. J. Engelsen, R. Krishnakumar, and M. A. Kasevich, *Nature* **529**, 505 (2016), URL <http://dx.doi.org/10.1038/nature16176>.
- [10] J. K. Stockton, Ph.D. thesis, California Institute of Technology (2007), URL <http://resolver.caltech.edu/CaltechETD:etd-02172007-172548>.
- [11] N. Behbood, G. Colangelo, F. Martin Ciurana, M. Napolitano, R. J. Sewell, and M. W. Mitchell, *Phys. Rev. Lett.* **111**, 103601 (2013), URL <http://link.aps.org/doi/10.1103/PhysRevLett.111.103601>.
- [12] I. H. Deutsch and P. S. Jessen, *Optics Communications* **283**, 681 (2010), ISSN 0030-4018, quo vadis Quantum Optics?, URL <http://www.sciencedirect.com/science/article/pii/S0030401809010517>.
- [13] J. Appel, P. J. Windpassinger, D. Oblak, U. B. Hoff, N. Kjærgaard, and E. S. Polzik, *Proc. Nat. Acad. Sci.* **106**, 10960 (2009), URL <http://www.pnas.org/content/106/27/10960.abstract>.
- [14] M. Koschorreck, M. Napolitano, B. Dubost, and M. W. Mitchell, *Phys. Rev. Lett.* **104**, 093602 (2010), URL <http://link.aps.org/doi/10.1103/PhysRevLett.104.093602>.
- [15] T. Takano, M. Fuyama, R. Namiki, and Y. Takahashi, *Phys. Rev. Lett.* **102**, 033601 (2009), URL <http://link.aps.org/doi/10.1103/PhysRevLett.102.033601>.
- [16] H. Hansen, T. Aichele, C. Hettich, P. Lodahl, A. I. Lvovsky, J. Mlynek, and S. Schiller, *Opt. Lett.* **26**, 1714 (2001), URL <http://ol.osa.org/abstract.cfm?URI=ol-26-21-1714>.
- [17] P. J. Windpassinger, M. Kubasik, M. Koschorreck, A. Boisen, N. Kjærgaard, E. S. Polzik, and J. H. Müller, *Measurement Science and Technology* **20**, 055301 (2009), URL <http://stacks.iop.org/0957-0233/20/i=5/a=055301>.
- [18] H. Mabuchi and N. Khaneja, *International Journal of Robust and Nonlinear Control* **15**, 647 (2005), ISSN 1099-1239, URL <http://dx.doi.org/10.1002/rnc.1016>.
- [19] H. Bachor and T. Ralph, *A Guide to Experiments in Quantum Optics* (Wiley, 2004), ISBN 9783527403936, URL <https://books.google.es/books?id=7yCLQgAACAAJ>.
- [20] M. Koschorreck, M. Napolitano, B. Dubost, and M. W. Mitchell, *Phys. Rev. Lett.* **104**, 093602 (2010), URL <http://link.aps.org/doi/10.1103/PhysRevLett.104.093602>.
- [21] M. Takeuchi, T. Takano, S. Ichihara, A. Yamaguchi, M. Kumakura, T. Yabuzaki, and Y. Takahashi, *Applied Physics B* **83**, 33 (2006), ISSN 1432-0649, URL <http://dx.doi.org/10.1007/s00340-006-2137-x>.